Detection of coastal flooding with TinyCamML: a low-cost, privacy-preserving cellular-connected camera with onboard ML

E. B. Farquhar[1], E. B. Goldstein[2], P. J. Bresnahan[3,4], B. Settin[3,4], J. Stasiewicz[2], K. Anarde[1]

[1]Department of Civil, Construction, and Environmental Engineering, North Carolina State University, Raleigh, NC, USA. [2]Sediment, Greensboro, NC, USA. [3]Department of Earth and Ocean Sciences, University of North Carolina at Wilmington, Wilmington, NC, USA. [3]Center for Marine Science, University of North Carolina at Wilmington, Wilmington, NC, USA

Corresponding author: Elizabeth Farquhar (efarquh@ncsu.edu)

Key Points:

- The TinyCamML is an open source, low-cost, privacy-preserving, real-time camera with an onboard binary classification ML model.
- The TinyCamML shows a 90% recall at identifying roadway floods in coastal settings, as seen during several compound flood events in NC, USA.
- The device can be easily modified to capture other rare or ephemeral environmental phenomena by retraining the onboard ML model.

Abstract

Chronic flooding is an issue for low-lying coastal communities globally, and it is expected to worsen with rising sea levels. In contrast to floods driven by extreme storms, predicting when and where these floods occur can be difficult as they can be hyper-local and short-lived, depending on the flood drivers (e.g., tides, rain). These factors make it difficult to measure the full spatial and temporal extent of chronic floods with in-situ sensors. Here, we introduce a low-cost (< $400 USD), privacy-preserving camera system that identifies flooding over block-by-block spatial extents at high frequencies (20 sec–6 min). Our device—a Tiny Camera with Machine Learning (TinyCamML)—is a small, solar-powered, microcontroller-based camera that uses on-device machine learning to classify images of roadways as containing a "flood" or "no flood." TinyCamMLs transmit only the classifications (a 1 or 0) to a website in real time, providing situation awareness during flood events over the entire image area while keeping data-transmission costs low and preserving privacy. We demonstrate the TinyCamML's utility during both tidal and compound flood events in North Carolina, USA, which showed differences in flood spatial extents. During this deployment, the TinyCamML detected floods with an 81% accuracy, a 72% precision, and a 90% recall. The utility of the device extends beyond roadway flooding, as the onboard machine learning model can be easily retrained to capture other rare or ephemeral phenomena.

Plain Language Summary

With rising sea levels, flooding is an increasing issue along low-lying coastlines all over the world. Depending on what causes the floods (e.g., tides or rain), they can be as small as puddles or span many blocks, and they may be composed of saltwater, which can degrade infrastructure and cars. Floods on roads are usually measured at a single point (e.g., in a drain, on the side of the road), which may not capture the full extent of the flood. Here we introduce a low-cost camera that can be used to automatically detect flooding across large sections of roadways in real time, without transmitting the full image. The camera has a built-in algorithm that uses machine learning to classify the image as containing a "flood" or "no flood." In this paper, we show how useful the camera is at detecting tidal and rain-driven floods; however, it could also be modified to identify other hazards, such as "Fire" or "No Fire."

1 Introduction

Coastal flooding is an increasing issue in low-lying communities across the world. It is estimated that 1.2 million people will be living below the high-tide line in the United States with 0.32–0.63 m of global mean sea-level rise (GMSL), which is the low to moderate emissions scenario for 2020 to 2100 (RCP 4.5; Church et al., 2014; Hauer et al., 2021). Before a community becomes permanently inundated, it will likely experience chronic flooding (Dahl et al., 2017).

Chronic flooding—or recurrent flooding that occurs outside of extreme storm events like tropical cyclones, Nor'easters, or atmospheric river events—can impact individuals and communities by limiting accessibility to important places such as homes, businesses, or

emergency facilities (Jacobs et al., 2018; Kasmalkar et al., 2024; Moftakhari et al., 2018). Exposure to contaminants such as fecal bacteria pose a human health risk (Carr et al., 2024; Price et al., 2021), and by influencing economic outcomes, such as loss in business revenues (Hino et al., 2019). The drivers and impacts of chronic flooding in coastal communities can be local—varying block-by-block—making it difficult to monitor and measure these floods with in-situ sensors (Gold et al., 2023). While the underlying driver of these floods is relative sea-level rise (which includes the effects of subsidence), regional differences in wind setup, tides, and river discharge can cause marine contributions to floods to vary regionally (Li et al., 2022; Sweet et al., 2018). Land-based factors, including groundwater, rainfall, and the condition of stormwater infrastructure (Loftis et al., 2018; Moftakhari et al., 2017; Thelen et al., 2024), also contribute to differences in flooding across communities. Tide gauges, which are used to infer flooding on land through point-based measurements in marine waterbodies, have been shown to be inadequate in capturing the frequency and duration of chronic floods, largely due to differences in land-based flood drivers (Hino et al., 2025). Hence, monitoring flooding at hyper-local scales, and on land, is critical to understanding the causes and impacts of chronic floods, as well as for informing infrastructure changes, policies, and risk management strategies (Albano et al., 2017; Van Alphen et al., 2009).

Several land-based sensor networks have already been leveraged to monitor chronic coastal flooding. Ultrasonic distance sensors have been deployed above roads and sidewalks in New York City to monitor roadway floods at a single point (FloodNet; Mydlarz et al., 2024), as well as in Texas (Ham et al., 2020). Similarly, ultrasonic sensor designs deployed in waterways can easily be adapted for roadway deployments (Bresnahan et al., 2023). The Sunny Day flood Sensors (SuDS; Gold et al., 2023), which consist of an in-situ pressure sensor housed within a storm drain and a subaerially mounted camera, have been used to monitor roadway floods across several communities in North Carolina (Hino et al., 2025; Thelen et al., 2024). The SuDS co-located camera and gateway is used for visual confirmation of flooding and real-time visual risk communication. Camera systems can potentially provide a wealth of information on flooding—such as spatial extent, impacts, or other auxiliary information—but the images typically require manual categorization to determine if an image contains a flood or not.

The use of machine learning (ML) on real-time images presents a fast way to automate the identification of floods from imagery to provide real-time information—information that would not be otherwise possible to obtain without a team of operators labeling images in real time or end-users deciding for themselves. ML cameras are already being utilized to monitor flooding; systems like FloodVISION-AI and AquaCam use cameras to estimate water levels near streams and waterways (Latham et al., 2025; Loftis et al., 2018). However, there exists a risk to privacy with any environmental monitoring systems using cameras—whether using ML or not. People and property are present in all images, and an automated system that could classify

images and report the results of the classification without storing or transmitting the image itself would help mitigate privacy concerns (e.g., Warden et al., 2023)

Here we combine camera data streams and ML for flood monitoring as a way to supplement or replace point-source measurements of floods with information about flooding across a larger field of view. Our device—the Tiny Camera with ML, or TinyCamML—uses on-board (edge) ML to classify images as containing a "flood" or "no flood." TinyCamMLs transmit only the classification—"flood" or "no flood"—to a website in real time, so images of roadways are not saved or transmitted, protecting the privacy of the local communities in which they are deployed. In this paper, we first provide information on the low-cost (<$400 USD) design of the TinyCamML and the development of the onboard ML model. We then demonstrate its use in classifying roadway floods during tidal and compound flood events. Finally, we discuss opportunities for alternative uses of the device, including monitoring other environmental phenomena.

2 TinyCamML Design

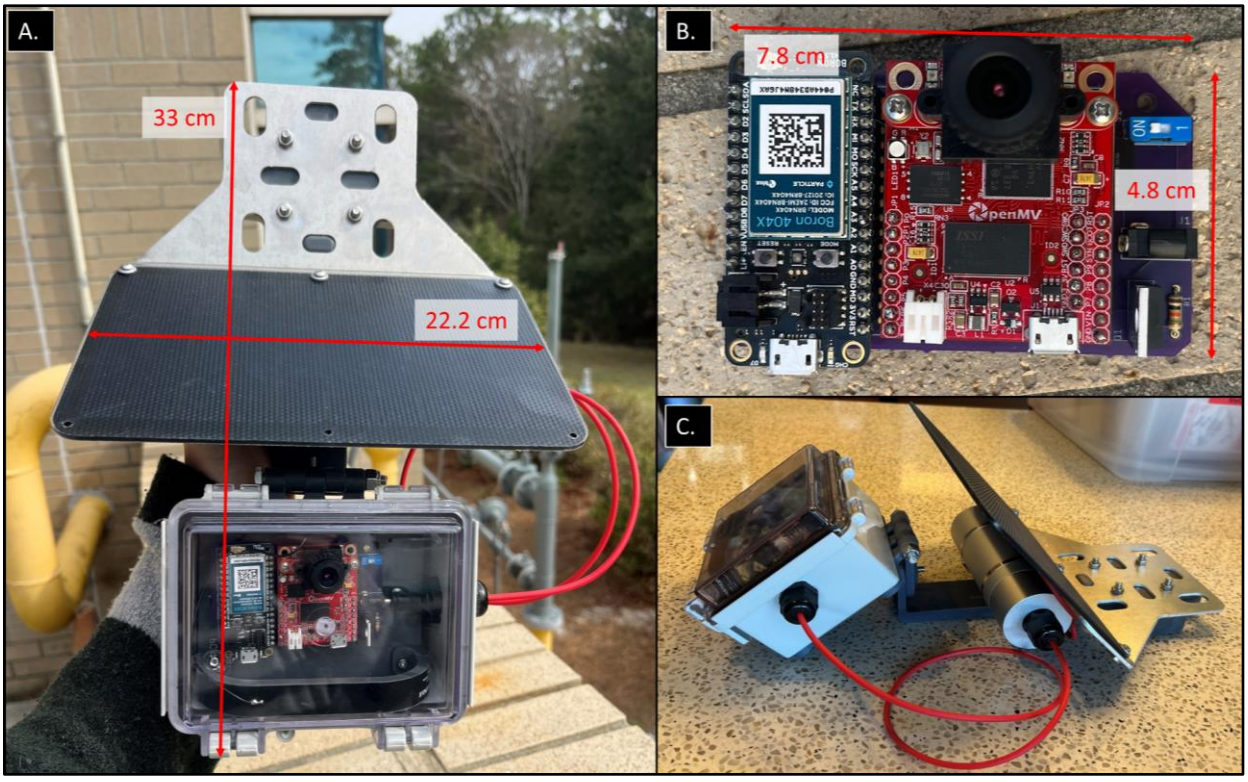

Figure 1. **a)** Fully assembled TinyCamML. **b)** The Boron and OpenMV Cam microcontrollers mounted onto the custom printed circuit board (purple). **c)** Side view of the fully assembled TinyCamML with Voltaic Systems solar panel and Polycase enclosure.

2.1 Electronics and housing

The TinyCamML hardware is composed of four parts: a 5W 5V solar panel and 5V 36Wh external battery (Voltaic Systems, Brooklyn, NY, USA), a Boron microcontroller with cellular connectivity (Particle, San Francisco, CA, USA), an OpenMV Cam H7 Plus microcontroller (OpenMV, Atlanta, GA, USA), and a MOSFET switch. The solar panel/battery powers the Boron, which in turn powers the OpenMV Cam as controlled by the MOSFET switch. The FET switch enables full depowering of the OpenMV Cam during sleep periods and robust synchronization of the Boron and OpenMV Cam at the beginning of a sampling cycle. All electrical components are secured onto a custom printed circuit board (PCB), which is fixed to a custom 3D-printed electronics tray and secured inside a Polycase enclosure (Polycase, Avon, OH, USA). The Polycase is fastened to the solar panel by a variety of 3D-printed parts. We use a Formlabs 3 SLA printer and Tough 2000 resin for all parts (Formlabs, Boston, MA, USA). Specific part numbers for all components, 3D designs, and a circuit diagram can be found on the TinyCamML GitHub repository (Farquhar et al., 2025).

2.2 Software

The TinyCamML software is designed so the system takes an image, passes the image through an onboard ML model, and then transmits the ML classification over cellular to a website for logging, as well as internally to a microSD card. These actions are accomplished with both microcontrollers: once woken, the OpenMV takes a photo and runs the ML model (via TensorFlow Lite Micro/LiteRT for Microcontrollers; David et al., 2021). The classification is then sent to the Boron over Universal Asynchronous Receiver/Transmitter (UART), and the Boron publishes a 1 or 0 to a Google sheet in real time. The Boron sends its timestamp data to the OpenMV Cam over UART, so the OpenMV Cam saves a timestamp with each ML classification in the data log. By default, images are not saved, but the OpenMV Cam can save images to its onboard microSD card. As discussed below, these images can be used to develop an image dataset for model training. Images are never transmitted, only classification scores. This saves on bandwidth and maintains privacy. Currently, the OpenMV Cam does not classify images when the scene brightness is below a threshold, which prevents unnecessary operation during low- and no- light conditions (i.e., night time), when accurate classifications are not currently possible. Source code for the Boron microcontroller was developed using the Particle Workbench extensions in Visual Studio Code version 1.95.3 and Particle's Device OS 6.1.0. OpenMV Cam source code was developed on the OpenMV IDE version 4.1.5 and system firmware v4.5.5. All source code is available on the TinyCamML GitHub repository (Farquhar et al., 2025).

2.3 ML classification model

The deep-learning based classifier model (herein referred to as the "classification model") that operates on the TinyCamML device was built using images from 3 sources: images

saved from deployed TinyCamML devices, imagery from SuDS cameras (Gold et al., 2023), and publicly-available datasets of roadway flooding (Chaudhaury et al., 2020, Sazara, 2019; Wang et al., 2024a, 2024b). These images were collected from different locations, vantages, and times of day. For the TinyCamML and SuDS imagery, we labeled images into two classes: a "flood" when the water extended across the crest of the roadway such that a car could not pass without going through water, and "no flood" to indicate any other condition. We elaborate on the potential implications of our definition of flooding further in the discussion. Our images were labeled by a single labeler for consistency, but we also performed an inter-rater agreement experiment with a subset of testing data; these results can be seen in Section 3 below. Our initial distribution of labeled images from the 3 datasets was strongly skewed toward non-flooded imagery. Therefore, to balance the dataset, we used ClimateGAN (Schmidt et al., 2021) on unflooded images to produce synthetic flood imagery. The use of synthetic imagery is a common tool to increase training data (Nikolenko 2021), especially for imbalanced datasets. In total, we assembled a dataset with 17,448 images, and a 50/50 split between "flood" and "no flood" images.

We train the classification model using TensorFlow (Abadi et al., 2016), leveraging the MobilenetV2 architecture (Sandler et al., 2018), and relying on ImageNet weights for the base model. We replace the classification head of the model with a global average pool, a dense layer with 1024 units, and a dense layer with 2 units (corresponding to our two classes, "flood" and "no flood"). The model accepts input images that are 224 x 224 pixels in dimension, and all 3 channels (red-green-blue). We use a dataset split of 60%, 25%, and 15% for training, validation, and testing (respectively). Other model specifications include early stopping, using categorical cross-entropy as the loss function, Adam as the optimizer (learning rate of $3x10^{-3}$), a dropout rate of 50% between the dense layers, a batch size of 16, an early stopping callback (patience of 10 epochs), image augmentations on the training data (rotation, width and height shift, shear, zoom, horizontal and vertical flips), and calculating the binary accuracy and a confusion matrix as a performance metric. During training, only the new classification layers are trainable. The trained model is then integer quantized using TensorFlow Lite micro (David et al., 2021) for inference on the OpenMV. The quantized model has a binary accuracy of 88% with the test set. The use of synthetic data can sometimes lead to reduction in performance during deployment (e.g., Liang et al., 2022), so it is critical to test the model further and demonstrate its effectiveness in the real world.

3 Demonstrating the TinyCamML's utility - November 2024

We demonstrate the utility of the TinyCamML in sensing roadway flooding during a series of floods in Carolina Beach, NC, that took place from November 14–18, 2024. Four

TinyCamMLs were deployed along a single roadway: Canal Drive. The floods were driven in part by perigean-spring tides (when the moon is either new or full and closest to Earth in its orbit), as well as rainfall. From November 11–18, 1.8 cm of precipitation fell across the region (as measured by the Coastal Ocean Research Monitoring Program Masonboro Island weather station, located about 5 km from Canal Drive), with 1.63 cm inches of rain falling on November 14 alone, which contributed to several compound flood events.

We compare the ML classification (e.g., “flood” or “no flood”) of each TinyCamML against user (visual) confirmation of flooding from each photo. As was the case in the training data, an image was labeled as “flooded” when the water extended across the crest of the road such that a car could not use the roadway without driving through water. The TinyCamMLs were deployed at three locations along a 1 km stretch of Canal Drive where there are existing water level sensors located in storm drains (i.e., part of the SuDS network; Gold et al., 2023). The water-level data from each gauge is plotted against the TinyCamML data in Figure 3 to provide context for flood depth and duration.

Figure 2. Example imagery from the TinyCamMLs in different flood conditions during November 14-18, 2024 along three different locations on Canal Drive in Carolina Beach, NC. TinyCamML 1 and 2 were at the same location facing different directions

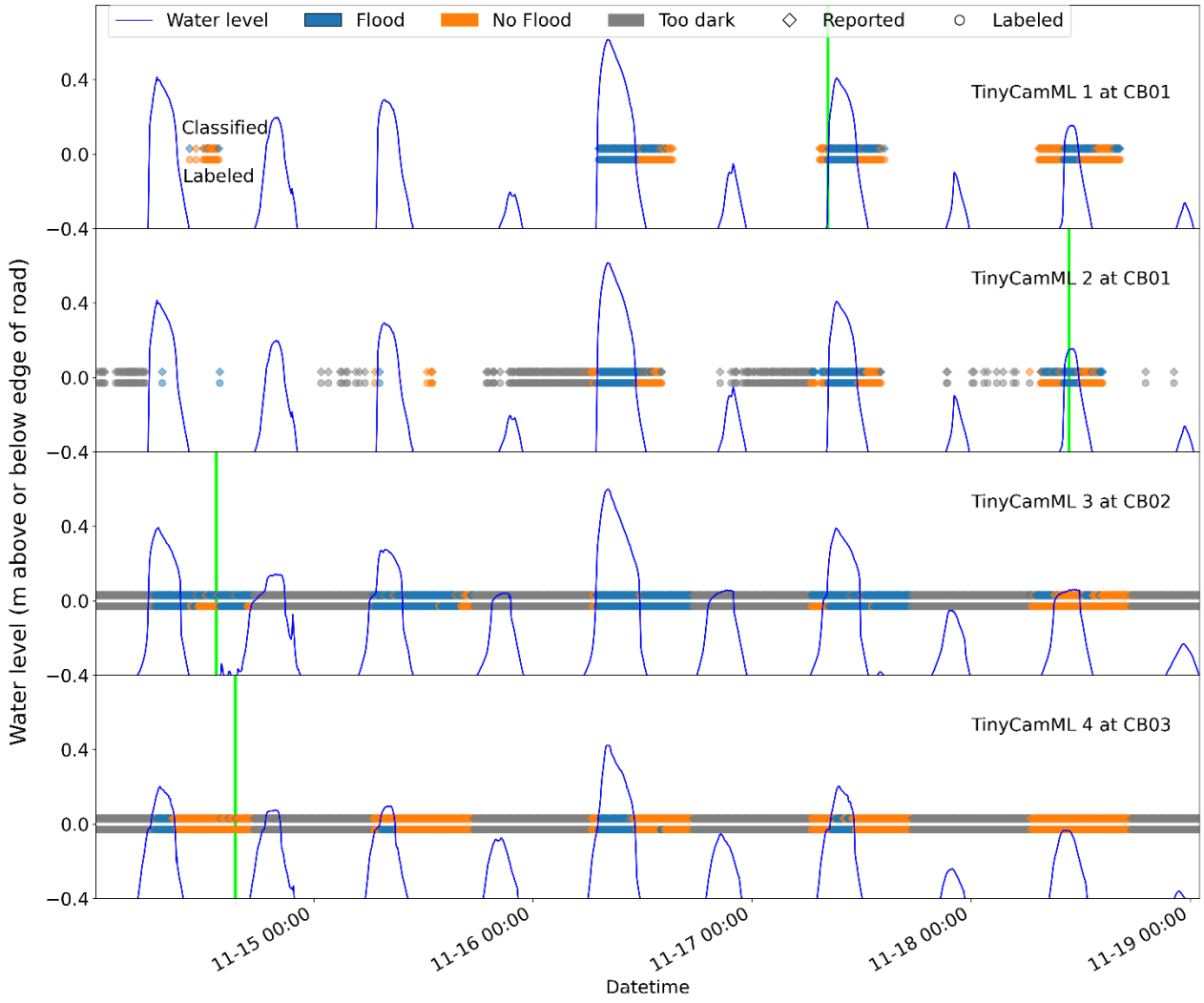

Figure 3. TinyCamML classifications compared with the user-labeled images, plotted against water levels above and below the edge of the pavement, recorded within storm drains (Gold et al., 2023). The green vertical lines indicate when the images in Figure 2 were taken.

Example imagery from the TinyCamMLs during various conditions throughout the deployment is shown to demonstrate the effect that environmental conditions (e.g., rain, sunlight) may have on the image classification (Figure 2). The photo in I shows a correct classification of “flood” by TinyCamML 2 during a clear sunny day (tidal flood event). In II, the image was taken at the transition between “no flood” and “flood,” where the floodwaters had just barely extended over the crest of the roadway on the right side of the photo (the yellow solid line). TinyCamML 1 classified this image as “no flood,” when labeler identification would consider this a “flood.” In III, there are puddles on the roadway that we do not consider to be a “flood” because they do not extend across the crest of the road, but TinyCamML 3 classified it as one. Image IV demonstrates how water droplets look when impeding the TinyCamML’s view

(compound rainfall event); however, despite this, TinyCamML 4 correctly classified this image as “no flood.”

We compare time series of water levels from SuDS sensors (mounted within storm drains) against the classifications of the TinyCamMLs and visually-confirmed user-labeled images (Figure 3). There are large gaps in the reporting records of TinyCamMLs 1 and 2 because they were earlier designs and therefore had issues with reporting consistency. Since then, all TinyCamMLs have been updated to the most recent design and are performing as expected. We include example imagery from TinyCamMLs 1 and 2 here because their field of view is distinctly different from the other cameras. Collectively, for the data shown in Figure 3, the TinyCamMLs classified images as “flooded” when there was a visually-confirmed flood 90% of the time, excluding “too dark” imagery. When there was not a visually-confirmed flood, the TinyCamMLs reported “flood” 26% of the time (i.e., a “false positive”).

We use a confusion matrix to further assess the performance of the ML model for the 1574 images taken during the November 14-18, 2024, deployment and show aggregate data as well as individual camera data (Figure 4). Across all four cameras, this deployment had an 81% accuracy, a 72% precision for detecting floods, and a 90% recall for detecting floods. When looking at all four cameras, the model was generally strong at predicting floods with only 66 false negatives (i.e., instances where there was flooding but the model predicted “no flood”). However, the model tended to overpredict flooding with 237 false positives (i.e., instances of no flooding where the model predicted “flood”). This general trend was seen in the data from TinyCamMLs 1-3. TinyCamML 4 had many false negatives and very few false positives.

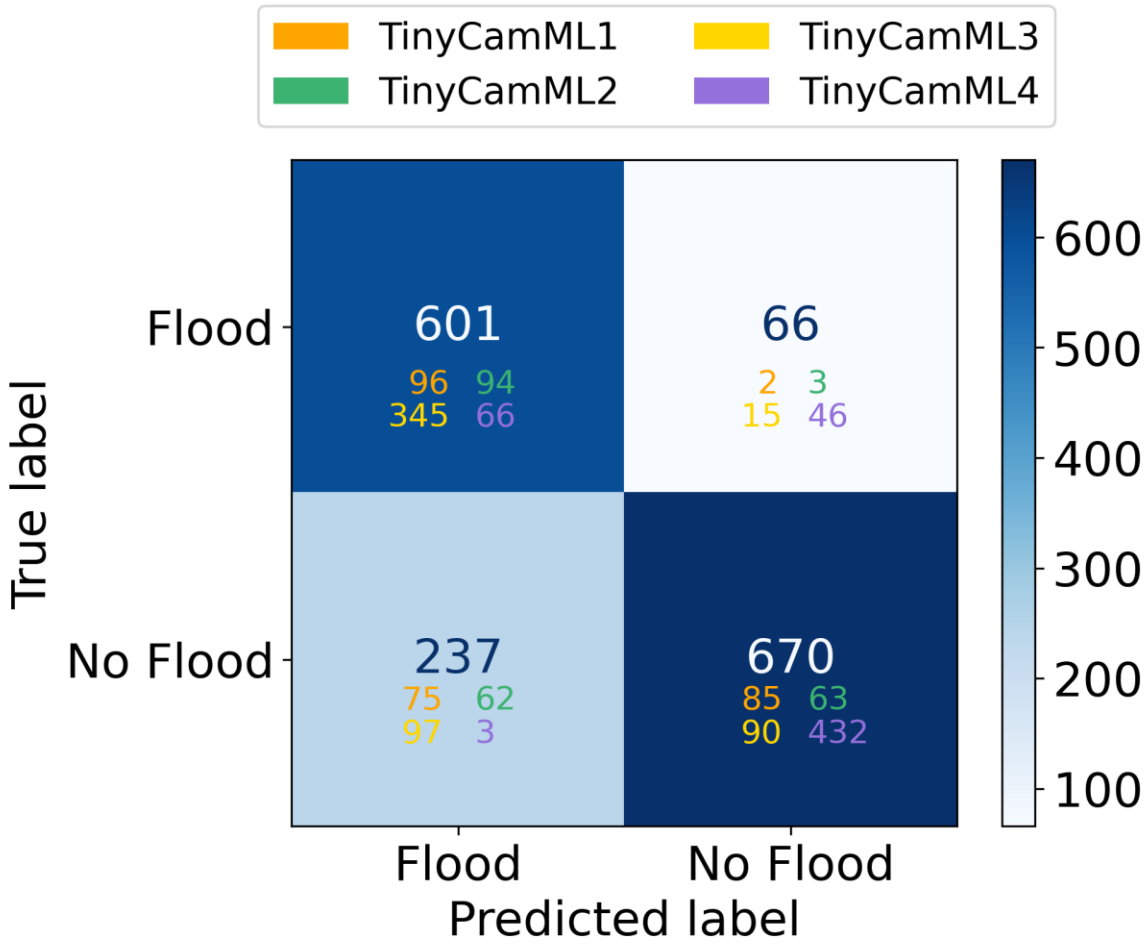

Figure 4. Confusion matrix of the classifications by the TinyCamMLs during the November 14-18, 2024 deployment. The larger number in each box indicates the sum of the number of classifications by each individual TinyCamML, which is color coded.

Lastly, we performed an inter-rater agreement experiment with two labelers for this dataset to better understand consistency in labels. This dataset and its labeling was not used for training the classification model. We used Krippendorff's Alpha to calculate agreement, where a score of -1 indicates no agreement, a score of 1 indicates total agreement, and a score of 0 being chance agreement (Krippendorff, 1970). TinyCamMLs 1-4 had a Krippendorff value of 0.98, 0.92, 0.59, and 0.94, respectively.

4 Discussion

Here we demonstrated the ability of the TinyCamML, a new open-source ML camera that both preserves privacy and offers low data transmission cost, in classifying roadway flooding under variable environmental conditions. Four TinyCamMLs deployed along a single road in Carolina Beach, NC, successfully identified flooding over a four day period 90% of the

time (as compared to visually-confirmed user-labeled images; Figure 3). However, the TinyCamMLs also reported false positives; the classification model reported flooding when there was not visually-confirmed flooding 26% of the time. The on-device ML model is continually being trained and improved upon, so we expect the number of false positives (and false negatives) shown in Figure 4 to decrease as more data is captured and used for training. Based on the confusion matrix, the models are generally performing in a manner where they do not miss detecting a flood (low false negatives), but tend to have false alarms (higher false positives). Depending on the specific deployment scenario, this may be more or less preferable.

The accuracy of the TinyCamML in predicting roadway floods was only calculated for a single definition of flooding – that is, when the water extended across the crest of the roadway such that a car could not pass without going through water. Using our definition of flooding, there were instances where the TinyCamMLs did detect water on the road and reported "flood," but because the water was not fully covering the roadway, the labeler determined those instances as "no flood," such as in image III of Figure 2. The TinyCamMLs reported false negatives 10% of the time, but again, many of these instances occurred during the transition between the roadway being dry to fully inundated at the centerline (Figure 2, image II). While the model performance is indeed sensitive to our chosen definition of flooding, the definition used here provides insight into when a roadway potentially becomes a depth hazard for vehicles (e.g., in 30-40 cm of water, a vehicle can float; Martínez-Gomariz et al., 2016), or for the case of tidal floods, when damage to vehicles is likely due to splashing from saltwater. Images that showed persistent puddles and/or this transition seem to be edge cases for the TinyCamML that will likely improve with further ML model training. Importantly, model accuracy, as well as the number of images needed to train the model to reach that accuracy, may differ for other definitions of flooding (e.g., any amount of ponding on the road, as used by Hino et al., 2025).

Overall model accuracy is also highly dependent on the deployment location and field of view. TinyCamML 3 had the highest individual percentage of false positives, but its field of view contained many large persistent puddles. As shown in Figure 3, TinyCamML 3 reported "flood" even after the water levels had receded because these puddles stayed on the roadway. For our interrater experiment with non-training data, TinyCamML 3 also had the lowest Krippendorff value (0.59) between labelers, which is likely also due to persistent puddles and the difficulty of determining exactly when the puddles connect enough to become classified as a flood. Despite this, a Krippendorff value of 0.59 is still comparable to other interrater agreement experiments in the coastal sciences (Goldstein et al., 2021). For the images from TinyCamMLs 1, 2, and 4, the labelers showed near complete agreement (0.98, 0.92, and 0.94), and these fields of view were typically devoid of persistent puddles.

More work is needed to determine how well our ML model generalizes to other environments that experience roadway flooding (e.g., in rural communities or more urban settings), and how the model accuracy might change under different environmental forcing conditions. Here, we showed that the TinyCamMLs can successfully classify roadway floods even during rainfall events when droplets obstruct the images (e.g., for TinyCamML 3 and 4 on November 14, 2024; Figure 3). It is unknown how changes in solar glare, shadows from large buildings, or vegetation changes may influence our model classifications and accuracy. Future deployments will be tailored toward development of a large, generalized training dataset with many different fields of view and spanning more environmental variables.

We envision several use cases for edge ML devices like the TinyCamML beyond spatial identification of roadway floods. First, since our device reports its classifications in real time to a website, and because the devices are low-cost, a network of TinyCamMLs can be used for real-time monitoring of transportation hazards. In the context of flooding, this type of sensor network could be used for real-time routing of emergency vehicles around flooded areas, and provide data to validate models of the impacts of flooding on road networks (e.g., Aldabet et al., 2022). The TinyCamML hardware and classification model can also be adapted to other monitoring and measuring tasks focused on difficult-to-observe, or ephemeral, environmental phenomena. In coastal settings, this could include binary classification of dune erosion, extreme run-up, impacts to structures, and other storm driven processes. In non-coastal settings, TinyCamMLs may be modified to observe extreme water levels in streams (similar to Latham et al., 2025 and Loftis et al., 2018), identify landslides, and early detection of wildfires (e.g., Shi et al., 2020), avalanches (e.g., Fox et al., 2024), or a range of other processes.

As coastal communities will experience more chronic flooding with rising sea levels, data on flood incidence, extent, and duration will become increasingly important for informing risk assessments and developing flood mitigation strategies (Albano et al., 2017; Van Alphen et al., 2009). The TinyCamML is an important advancement in low-cost, privacy preserving monitoring technology that enables identification of flooding in places where investment in in-situ sensors may not have been historically prioritized: on land or in residential areas, where people interact with floodwaters most.

Acknowledgments

This work has been supported by the National Aeronautics and Space Administration through Grant 80NSSC24K0504. The authors thank Jeremy Hardison and Daniel Keating with the Town of Carolina Beach for their support in deployment of the TinyCamMLs. We also thank several senior design teams at NC State University for developing alternate prototypes of the TinyCamML that helped refine the final camera design. We thank Joe Bolewitz for some preliminary data labeling and Matthew Saenz for his assistance in designing the PCB. The

CORMP weather data included in this publication was prepared using data provided to the University of North Carolina Wilmington under award NA21NOS0120097 from the National Oceanic and Atmospheric Administration, U.S. Department of Commerce. The statements, findings, conclusions, and recommendations are those of the author{s) and do not necessarily reflect the views of the National Oceanic and Atmospheric Administration or the Department of Commerce.

Open Research

The build guide for the TinyCamML, the designs of the 3D printed parts, hardware descriptions, source code files, and machine learning models can all be found in the TinyCamML V0.2 repository on the Github page, archived in Zenodo (Farquhar et al., 2025). The Github repository is under the MIT license and fully accessible. Additionally, the dataset used to train the machine learning models can be found on Zenodo (Goldstein et al., 2025).

References

Abadi, M., Agarwal, A., Barham, P., Brevdo, E., Chen, Z., Citro, C., Corrado, G. S., Davis, A., Dean, J., Devin, M., Ghemawat, S., Goodfellow, I., Harp, A., Irving, G., Isard, M., Jia, Y., Jozefowicz, R., Kaiser, L., Kudlur, M., … Zheng, X. (2016). *TensorFlow: Large-Scale Machine Learning on Heterogeneous Distributed Systems* (Version 2). arXiv. https://doi.org/10.48550/ARXIV.1603.04467

Albano, R., Mancusi, L., & Abbate, A. (2017). Improving flood risk analysis for effectively supporting the implementation of flood risk management plans: The case study of "Serio" Valley. *Environmental Science & Policy*, *75*, 158–172. https://doi.org/10.1016/j.envsci.2017.05.017

Aldabet, S., Goldstein, E. B., & Lazarus, E. D. (2022). Thresholds in Road Network Functioning on US Atlantic and Gulf Barrier Islands. *Earth's Future*, *10*(5), e2021EF002581. https://doi.org/10.1029/2021EF002581

Bresnahan, P., Briggs, E., Davis, B., Rodriguez, A. R., Edwards, L., Peach, C., Renner, N., Helling, H., & Merrifield, M. (2023). A LOW-COST, DIY ULTRASONIC WATER LEVEL SENSOR FOR EDUCATION, CITIZEN SCIENCE, AND RESEARCH. *Oceanography*, *36*(1), 51–58. JSTOR.

Carr, M. M., Gold, A. C., Harris, A., Anarde, K., Hino, M., Sauers, N., Da Silva, G., Gamewell, C., & Nelson, N. G. (2024). Fecal Bacteria Contamination of Floodwaters and a Coastal Waterway From Tidally-Driven Stormwater Network Inundation. *GeoHealth*, *8*(4), e2024GH001020. https://doi.org/10.1029/2024GH001020

Chaudhary, P., D'Aronco, S., Leitão, J. P., Schindler, K., & Wegner, J. D. (2020). Water level prediction from social media images with a multi-task ranking approach. ISPRS Journal of Photogrammetry and Remote Sensing, 167, 252–262. https://doi.org/10.1016/j.isprsjprs.2020.07.003

Church, P., Clark, P. U., & Cazenave, A. (2014). *Climate change 2013: The physical science basis: Working Group I contribution to the Fifth assessment report of the Intergovernmental Panel on Climate Change*. Cambridge University Press.

https://doi.org/10.1017/CBO9781107415324

Dahl, K. A., Spanger-Siegfried, E., Caldas, A., & Udvardy, S. (2017). Effective inundation of continental United States communities with 21st century sea level rise. *Elementa: Science of the Anthropocene*, *5*, 37. https://doi.org/10.1525/elementa.234

David, R., Duke, J., Jain, A., Reddi, V. J., Jeffries, N., Li, J., Kreeger, N., Nappier, I., Natraj, M., Wang, T., Warden, P., & Rhodes, R. (2021). TensorFlow Lite Micro: Embedded Machine Learning for TinyML Systems. *Machine Learning and Systems*, *3*. https://proceedings.mlsys.org/paper_files/paper/2021/hash/6c44dc73014d66ba49b28d483a8f8b0d-Abstract.html

Farquhar, E., Bentley Settin, Evan B. Goldstein, Jacob Stasiewicz, Matthew Saenz, & Phil Bresnahan. (2025). *TinyCamML/TinyCamML: V0.2* (Version V0.2) [Computer software]. Zenodo. https://doi.org/10.5281/ZENODO.15019916

Fox, J., Siebenbrunner, A., Reitinger, S., Peer, D., & Rodríguez-Sánchez, A. (2024). Automating avalanche detection in ground-based photographs with deep learning. *Cold Regions Science and Technology*, *223*, 104179. https://doi.org/10.1016/j.coldregions.2024.104179

Gold, A., Anarde, K., Grimley, L., Neve, R., Srebnik, E. R., Thelen, T., Whipple, A., & Hino, M. (2023). Data From the Drain: A Sensor Framework That Captures Multiple Drivers of Chronic Coastal Floods. *Water Resources Research*, *59*(4), e2022WR032392. https://doi.org/10.1029/2022WR032392

Goldstein, E. B., Buscombe, D., Lazarus, E. D., Mohanty, S. D., Rafique, S. N., Anarde, K. A., Ashton, A. D., Beuzen, T., Castagno, K. A., Cohn, N., Conlin, M. P., Ellenson, A., Gillen, M., Hovenga, P. A., Over, J. R., Palermo, R. V., Ratliff, K. M., Reeves, I. R. B., Sanborn, L. H., … Williams, H. E. (2021). Labeling Poststorm Coastal Imagery for Machine Learning: Measurement of Interrater Agreement. *Earth and Space Science*, *8*(9), e2021EA001896. https://doi.org/10.1029/2021EA001896

Goldstein, E.B., Farquhar, E.B., Anarde, K.A. (2025). Dataset for Detection of coastal flooding with TinyCamML: a low-cost, privacy-preserving cellular-connected camera with onboard ML. https://doi.org/10.5281/zenodo.16740295

Ham, S., Noh, S., Seo, D.-J., Kang, S., & David Dafnik Saril, K. (2020). *Real-Time Early Detection and Monitoring of Flooding Using Low-Cost Highly Sensitivity Ultrasound Sensing of Water Level* (Tech Report No. 19SAUTA03; pp. 1–42). Transportation Consortium of South-Central States (Tran-SET); Louisiana State University (Baton Rouge, La.); United States Department of Transportation; University Transportation Centers (UTC) Program. https://rosap.ntl.bts.gov/view/dot/58927

Hauer, M., Hardy, D., Kulp, S. A., Mueller, V., Wrathall, D. J., & Clark, P. U. (2021). Assessing population exposure to coastal flooding due to sea level rise. *Nature Communications*, *12*(1), 6900. https://doi.org/10.1038/s41467-021-27260-1

Hino, M., Anarde, K., Fridell, T., McCune, R., Thelen, T., Farquhar, E., Woodard, P., & Whipple, A. (2025). Land-based sensors reveal high frequency of coastal flooding. *Communications Earth & Environment*, *6*(1). https://doi.org/10.1038/s43247-025-02326-w

Hino, M., Belanger, S. T., Field, C. B., Davies, A. R., & Mach, K. J. (2019). High-tide flooding disrupts local economic activity. *Science Advances*, *5*(2), eaau2736. https://doi.org/10.1126/sciadv.aau2736

Jacobs, J. M., Cattaneo, L. R., Sweet, W., & Mansfield, T. (2018). Recent and Future Outlooks for Nuisance Flooding Impacts on Roadways on the U.S. East Coast. *Transportation Research Record*, *2672*(2), 1–10. https://doi.org/10.1177/0361198118756366

Kasmalkar, I., Wagenaar, D., Bill-Weilandt, A., Choong, J., Manimaran, S., Lim, T. N., Rabonza, M., & Lallemant, D. (2024). Flow-tub model: A modified bathtub flood model with hydraulic connectivity and path-based attenuation. *MethodsX*, *12*, 102524. https://doi.org/10.1016/j.mex.2023.102524

Krippendorff, K. (1970). Estimating the Reliability, Systematic Error and Random Error of Interval Data. *Educational and Psychological Measurement*, *30*(1), 61–70. https://doi.org/10.1177/001316447003000105

Latham, J., Dadzie, G., Kalyanapu, A., & Shannigrahi, S. (2025). AquaCam: An ML-Enhanced Low-Cost, Deploy-Anywhere Water Level Detection Sensor. *2025 IEEE International Conference on Pervasive Computing and Communications Workshops and Other Affiliated Events (PerCom Workshops)*, 628–632. https://doi.org/10.1109/percomworkshops65533.2025.00149

Li, S., Wahl, T., Barroso, A., Coats, S., Dangendorf, S., Piecuch, C., Sun, Q., Thompson, P., & Liu, L. (2022). Contributions of Different Sea-Level Processes to High-Tide Flooding Along the U.S. Coastline. *Journal of Geophysical Research: Oceans*, *127*(7). https://doi.org/10.1029/2021jc018276

Liang, W., Tadesse, G. A., Ho, D., Fei-Fei, L., Zaharia, M., Zhang, C., & Zou, J. (2022). Advances, challenges and opportunities in creating data for trustworthy AI. Nature

Loftis, D., Forrest, D., Katragadda, S., Spencer, K., Organski, T., Nguyen, C., & Rhee, S. (2018). StormSense: A New Integrated Network of IoT Water Level Sensors in the Smart Cities of Hampton Roads, VA. *Marine Technology Society Journal*, *52*, 10.4031/MTSJ.52.2.7. https://doi.org/10.4031/MTSJ.52.2.7

Martínez-Gomariz, E., Gómez, M., Russo, B., & Djordjević, S. (2016). Stability criteria for flooded vehicles: A state-of-the-art review. Journal of Flood Risk Management, 11(S2), S817–S826. https://doi.org/10.1111/jfr3.12262

Moftakhari, H. R., AghaKouchak, A., Sanders, B. F., Allaire, M., & Matthew, R. A. (2018). What Is Nuisance Flooding? Defining and Monitoring an Emerging Challenge. *Water Resources Research*, *54*(7), 4218–4227. https://doi.org/10.1029/2018WR022828

Moftakhari, H. R., AghaKouchak, A., Sanders, B. F., & Matthew, R. A. (2017). Cumulative hazard: The case of nuisance flooding. *Earth's Future*, *5*(2), 214–223. https://doi.org/10.1002/2016EF000494

Mydlarz, C., Sai Venkat Challagonda, P., Steers, B., Rucker, J., Brain, T., Branco, B., Burnett, H. E., Kaur, A., Fischman, R., Graziano, K., Krueger, K., Hénaff, E., Ignace, V., Jozwiak, E., Palchuri, J., Pierone, P., Rothman, P., Toledo-Crow, R., & Silverman, A. I. (2024). FloodNet: Low-Cost Ultrasonic Sensors for Real-Time Measurement of Hyperlocal, Street-Level Floods in New York City. *Water Resources Research*, *60*(5), e2023WR036806. https://doi.org/10.1029/2023WR036806

Nikolenko, S. I. (2021). Synthetic Data for Deep Learning (Vol. 174). Springer International Publishing. https://doi.org/10.1007/978-3-030-75178-4

Price, M. T., Blackwood, A. D., & Noble, R. T. (2021). Integrating culture and molecular quantification of microbial contaminants into a predictive modeling framework in a low-

lying, tidally-influenced coastal watershed. *Science of The Total Environment*, *792*, 148232. https://doi.org/10.1016/j.scitotenv.2021.148232

Sandler, M., Howard, A., Zhu, M., Zhmoginov, A., & Chen, L.-C. (2018). MobileNetV2: Inverted Residuals and Linear Bottlenecks. *CVPR 2018 Open Access*. https://openaccess.thecvf.com/content_cvpr_2018/html/Sandler_MobileNetV2_Inverted_Residuals_CVPR_2018_paper.html

Sazara, C. (2019). *Image Dataset for Roadway Flooding* [Dataset]. Mendeley. https://doi.org/10.17632/T395BWCVBW.1

Schmidt, V., Luccioni, A. S., Teng, M., Zhang, T., Reynaud, A., Raghupathi, S., Cosne, G., Juraver, A., Vardanyan, V., Hernandez-Garcia, A., & Bengio, Y. (2021). *ClimateGAN: Raising Climate Change Awareness by Generating Images of Floods*. https://doi.org/10.48550/ARXIV.2110.02871

Shi, J., Wang, W., Gao, Y., & Yu, N. (2020). Optimal Placement and Intelligent Smoke Detection Algorithm for Wildfire-Monitoring Cameras. *IEEE Access*, *8*, 72326–72339. https://doi.org/10.1109/ACCESS.2020.2987991

Sweet, W. V., Obeysekera, J. T. B., Marra, J. J., & Dusek, G. (2018). *Patterns and projections of high tide flooding along the U.S. coastline using a common impact threshold.* [PDF]. https://doi.org/10.7289/V5/TR-NOS-COOPS-086

Thelen, T., Anarde, K., Dietrich, J. C., & Hino, M. (2024). Wind and rain compound with tides to cause frequent and unexpected coastal floods. *Water Research*, 122339. https://doi.org/10.1016/j.watres.2024.122339

Van Alphen, J., Martini, F., Loat, R., Slomp, R., & Passchier, R. (2009). Flood risk mapping in Europe, experiences and best practices. *Journal of Flood Risk Management*, *2*(4), 285–292. https://doi.org/10.1111/j.1753-318X.2009.01045.x

Wang, Y. (2024). Urban Flood Image Dataset, HydroShare, http://www.hydroshare.org/resource/24866122a6ee456c8f7c80aa87a9abcb

Wang, Y., Shen, Y., Salahshour, B., Cetin, M., Iftekharuddin, K., Tahvildari, N., Huang, G., Harris, D. K., Ampofo, K., & Goodall, J. L. (2024). Urban flood extent segmentation and evaluation from real-world surveillance camera images using deep convolutional neural network. Environmental Modelling & Software, 173, 105939. https://doi.org/10.1016/j.envsoft.2023.105939

Warden, P., Stewart, M., Plancher, B., Katti, S., & Reddi, V. J. (2023). Machine Learning Sensors. *Communications of the ACM*, *66*(11), 25–28. https://doi.org/10.1145/3586991